



先端放射光源に関する研究会
岡崎コンファレンスセンター
2014年11月21日

回折限界光源から発する 軌道角運動量を持つ光とその応用

佐々木 茂美
広大放射光センター

On behalf of

佐々木茂美¹, 宮本篤¹, 加藤政博², 許斐太郎²,
保坂将人³, 山本尚人³, 今園孝志⁴, 小池雅人⁴

¹広大HiSOR, ²分子研UVSOR, ³名大SR, ⁴原子力機構量子ビーム

Outline

- ◆ 光渦：波動方程式の解
Light vortices: solutions to the wave equation
- ◆ 円偏光アンジュレータからの放射光
Synchrotron radiation from helical undulators
- ◆ UVSORでの実験について
Experiments at UVSOR
- ◆ 新奇な性質の利用可能性について
Possibility for using novel properties





$$\nabla \cdot \mathbf{E} = 0 \qquad \nabla \times \mathbf{E} + \frac{1}{c} \frac{\partial \mathbf{B}}{\partial t} = 0$$

$$\nabla \cdot \mathbf{B} = 0 \qquad \nabla \times \mathbf{B} - \frac{1}{c} \frac{\partial \mathbf{E}}{\partial t} = 0$$

source-free,
in vacuum

$$\mathbf{S} = \frac{c}{4\pi} \mathbf{E} \times \mathbf{B}$$

$$\mathbf{J} = \frac{1}{4\pi c} \int \mathbf{r} \times (\mathbf{E} \times \mathbf{B}) d\mathbf{r}$$

Poynting vector

Total angular momentum

$$\mathbf{J} = \frac{1}{4\pi c} \int \left[\underbrace{(\mathbf{E} \times \mathbf{A})}_{\text{Spin } S} + \sum_{i=1}^3 \underbrace{E_i (\mathbf{r} \times \nabla)}_{\text{Orbital } L} \right] d\mathbf{r}$$

where $\mathbf{B} = \nabla \times \mathbf{A}$

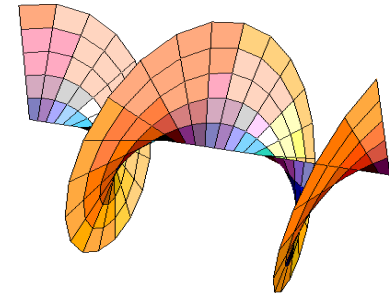
Spin S

Orbital L

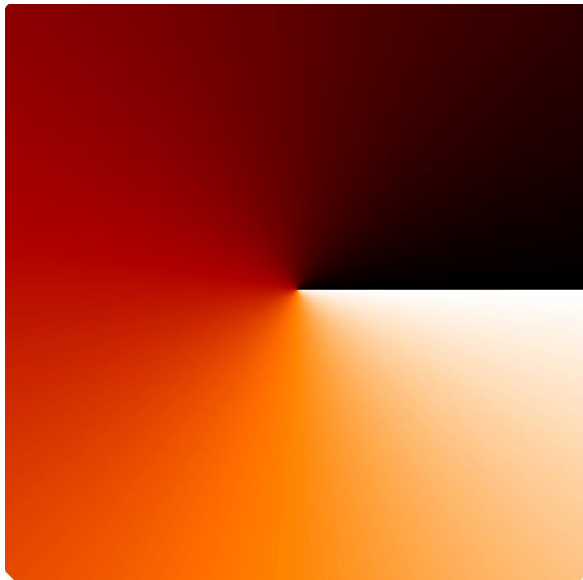


- Laguerre-Gaussian mode (azimuthal phase):

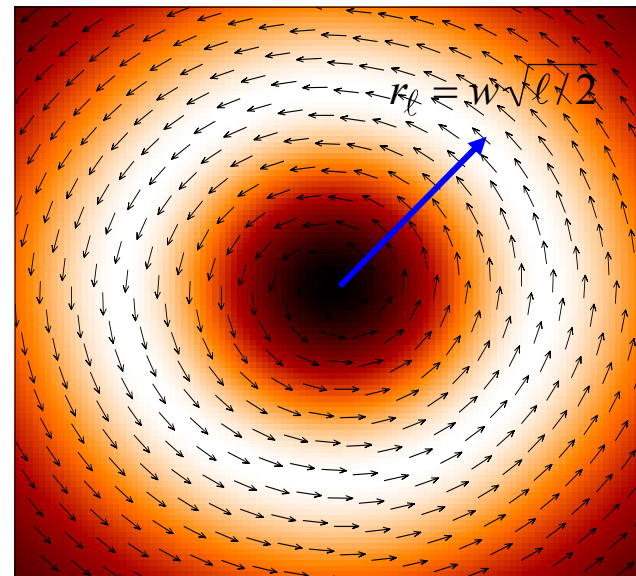
$$a_p^l(r, \phi, z) = A_p^l(r, z) \exp[-i\Phi_p^l(r, z)] \exp(-il\phi)$$



- The Poynting vector completely specifies the field



Phase



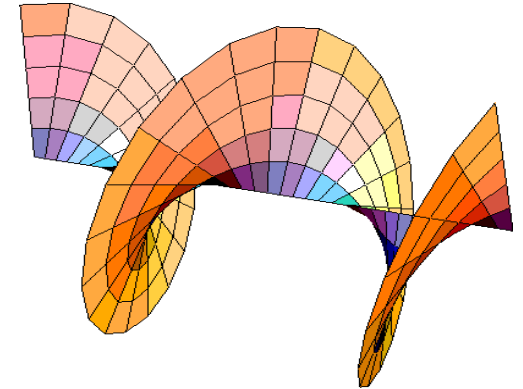
Magnitude



Phase singularities

Laguerre-Gaussian beams

- On-axis singularity characterized by helical phase front
- Poynting vector follows wavefront as beam propagates
- Gives rise to orbital momentum component
- Intensity is zero on-axis (optical donut)



Orbital angular momentum

- Distinct from spin AM associated with circular polarization
- Has magnitude of $\ell\hbar$ per photon, where topological "charge" ℓ is number of $(2\pi\ell)$ phase cycles around beam

$$L = \ell\hbar$$

$$(\ell = \text{integer})$$



Photon angular momentum

If every polarization vector rotates the light has spin.

If the phase structure rotates the light has orbital angular momentum

- M. Padgett

Spin

Orbital

linear/circular
axis-independent
intrinsic

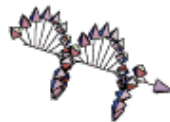
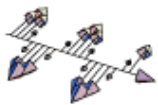
azimuthal
axis-dependent
intrinsic or extrinsic
(on-axis) (off-axis)

$$S = 0$$

$$S = \pm 1\hbar$$

$$L = 0$$

$$L = \ell \hbar$$



$$J = L + S$$



Light's Orbital Angular Momentum

The realization that light beams can have quantized orbital angular momentum in addition to spin angular momentum has led, in recent years, to novel experiments in quantum mechanics and new methods for manipulating microparticles.

Miles Padgett, Johannes Courtial, and Les Allen

Like all wave phenomena, light has mechanical properties. Johannes Kepler suggested that comet tails always point away from the Sun because light carries linear momentum. In 1905, John Poynting developed the theory of electromagnetic radiation pressure and momentum density and, in 1921, Albert Einstein showed that Planck's blackbody law and the motion of molecules in a radiation field could be explained if the linear momentum of a photon is $h\mathbf{k}$. (The wave number $k = 2\pi/\lambda$ and $h = h/2\pi$, where λ is the wavelength and h is Planck's constant.) In modern times, light's linear momentum has been directly exploited for trapping and cooling atoms and molecules.

It was also Poynting who, in 1909, realized that polarized light has angular momentum—spin angular momentum, associated with circular polarization. For a single photon, it has a value of $\pm\hbar$. The idea of light's orbital angular momentum came only much later. In 1992, a group at Leiden University in the Netherlands that included one of us (Allen) recognized that light beams with an azimuthal phase dependence of $\exp(-i\ell\phi)$ carries an angular momentum independent of the polarization state.¹ The angle ϕ is the azimuthal coordinate in the beam's cross section, and ℓ can take any integer value, positive or negative. This orbital angular momentum, they predicted, would have a value of $L = \ell\hbar$ per photon. Just as with circularly polarized light, the sign of the orbital angular momentum indicates its handedness with respect to the beam direction.

For any given ℓ , the beam has ℓ intertwined helical phase fronts, as illustrated in figure 1. A feature of helically phased beams is that the phase singularity on the beam axis dictates zero intensity on the axis. Therefore the cross-sectional intensity pattern of all such beams has an annular character that persists no matter how tightly the beam is focused. The on-axis singularity is a specific instance of phase dislocation, the general literature for which is recent, extensive, and beyond the scope of this article.²

The concept of optical orbital angular momentum of light is not altogether new. It is well known that multipolar transitions can produce radiation that carries orbital angular momentum. But such processes are rare and relate, in the visible, to a few "forbidden" atomic and molec-

ular transitions. What's new and exciting is that it is now possible to produce, rather easily, laboratory light beams with quantized orbital angular momentum. This can be used to investigate all the analogues of polarized light. For example, one can look for a photon analogue of the spin-orbit coupling of electrons and, quite generally, to search for new optical interactions.

Optical angular momentum

To a considerable extent, one can understand light's momentum properties without reference to photons. A careful analytic treatment of the electromagnetic field gives the total angular momentum of any light field in terms of a sum of spin and orbital contributions.³ In free space, the Poynting vector, which gives the direction and magnitude of the momentum flow, is simply the vector product of the electric and magnetic field intensities. For helical phase fronts, the Poynting vector has an azimuthal component, as shown in figure 1. That component produces an orbital angular momentum parallel to the beam axis. Because the momentum circulates about the beam axis, such beams are said to contain an optical vortex.

The most common form of helically phased beam is the so-called Laguerre-Gaussian (LG) laser mode. In general, lasers emit a beam that gradually expands as it propagates. The magnitude and phase of the electric field at different positions in the cross section are described by a mode function. For most laser beams without helical phasing, that function is the product of a Hermite polynomial and a Gaussian. Hermite-Gaussian (HG) modes have several intensity maxima, depending on the order of the polynomials, arrayed in a rectangular pattern and separated by intensity zeros.

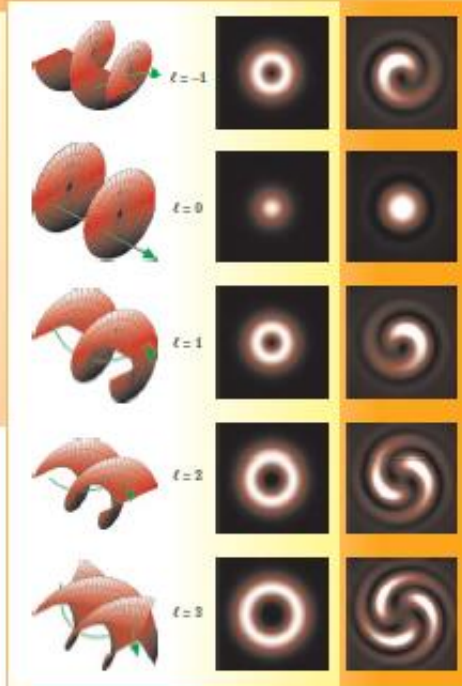
The cylindrical LG modes have an explicit $\exp(-i\ell\phi)$ phase factor. That makes them the natural choice for the description of beams carrying orbital angular momentum. Although LG modes have been produced directly in laser systems,⁴ they are more easily produced by the conversion of HG beams.

Generating the beams

Spin angular momentum depends only on the polarization of the beam, not on its phase. Therefore both HG and LG beams can possess spin angular momentum. Beams carrying spin angular momentum are readily produced by using a quarter-wave plate to convert linearly into circularly polarized light. The Leiden group introduced an analogous trick with cylindrical lenses to transform an HG beam with no angular momentum into a LG beam that carries orbital angular momentum (see figure 2).⁴

Although this conversion process is highly efficient, each LG mode does require a particular initial HG mode. That requirement limits the range of LG modes one can produce. Consequently, the most common method for cre-

Figure 1. Orbital angular momentum of a light beam, unlike spin angular momentum, is independent of the beam's polarization. It arises from helical phase fronts (left column), at which the Poynting vector (green arrows) is no longer parallel to the beam axis. At any fixed radius within the beam, the Poynting vector follows a spiral trajectory around the axis. Rows are labeled by ℓ , the orbital angular-momentum quantum number. $L = \ell\hbar$ is the beam's orbital angular momentum per photon. For each ℓ , the left column is a schematic snapshot of the beam's instantaneous phase. At a instant later, the phase advance is indistinguishable from a small rotation of the beam. By themselves, beams with helical wavefronts have simple annular intensity profiles (center column). But when such a beam is made to interfere with a plane wave, it produces a helical spiral intensity pattern (right column). The number of spiral arms equals the number ℓ of intertwined helical phase fronts of the helical beam.



ating helical beams has been the use of numerically computed holograms. Such holograms can generate beams with any desired value of orbital angular momentum from the same initial beam (see figure 3). The requisite hologram can be formed by recording, onto photographic film, the interference pattern between a plane wave and the beam one seeks to produce. Illuminating the resulting hologram with another plane wave produces a first-order diffracted beam with the intensity and phase pattern of the desired beam.

The holographic approach can take advantage of the high-quality spatial light modulators (SLMs) that have recently become available. These pixelated liquid-crystal devices take the place of the photographic film. Furthermore, numerically calculated holographic patterns can be displayed on an SLM. These devices produce reconfigurable, computer-controlled holograms that allow a simple laser beam to be converted into an exotic beam with almost any desired phase and amplitude structure. And the beam pattern can be changed many times per second to meet experimental requirements. Figure 3 shows how a comparatively simple "forked" holographic pattern can transform the plane-wave output of a conventional laser into a pair of LG beams carrying orbital angular momentum.⁵ In recent years, SLMs have been used in applications as diverse as adaptive optics, real-time holography, and optical tweezing.

Unlike spin angular momentum, which has only two independent states corresponding to left- and right-handed circular polarization, orbital angular momentum has an unlimited number of possible states, corresponding to all integer values of ℓ . Although the link between spin angular momentum and circular polarization is clear, the link between orbital angular momentum and other ways of describing the beam is less obvious. It's tempting, for example, to directly associate the orbital component to the ℓ value of an optical vortex; but that's wrong. Because the center of the vortex is a position of zero optical intensity, it carries neither linear nor angular momentum. Instead,

the angular momentum is associated with regions of high intensity, which for an LG mode is a bright annular ring.

That association is well illustrated by a recent experiment by Lluís Torner and coworkers at the University of Catalonia in Barcelona, Spain.⁶ They showed that, after the beam passes through the focus of a cylindrical lens, the azimuthal component of the linear momentum near the vortex center is reversed, but the total orbital angular momentum of the beam remains unchanged. The reversal of the vortex is simply image inversion in geometrical optics; it has no implications for orbital angular momentum.

Orbital angular momentum arises whenever a beam's phase fronts are not perpendicular to the propagation direction. In the approximation of geometric optics, one would say that the light rays that make up the beam are skewed with respect to its axis. Stipitistic as it is, this skewed-ray model predicts the correct result in most experimental situations.

Measuring the angular momentum of a light beam is not easy. The first demonstration of the transfer of spin angular momentum from a light beam was carried out in 1936 by Richard Beth at Princeton University.⁷ The experiment was extremely demanding. A suspended quarter-wave plate took angular momentum from a circularly polarized beam. The plate's macroscopic size and corresponding high moment of inertia, however, meant

Miles Padgett and Johannes Courtial are physicists at Glasgow University in Scotland. Les Allen holds visiting appointments at the Universities of Glasgow, Strathclyde, and Sussex.



Can we produce an *x-ray vortex*?

Need:

Intense, highly coherent X-ray or VUV beam

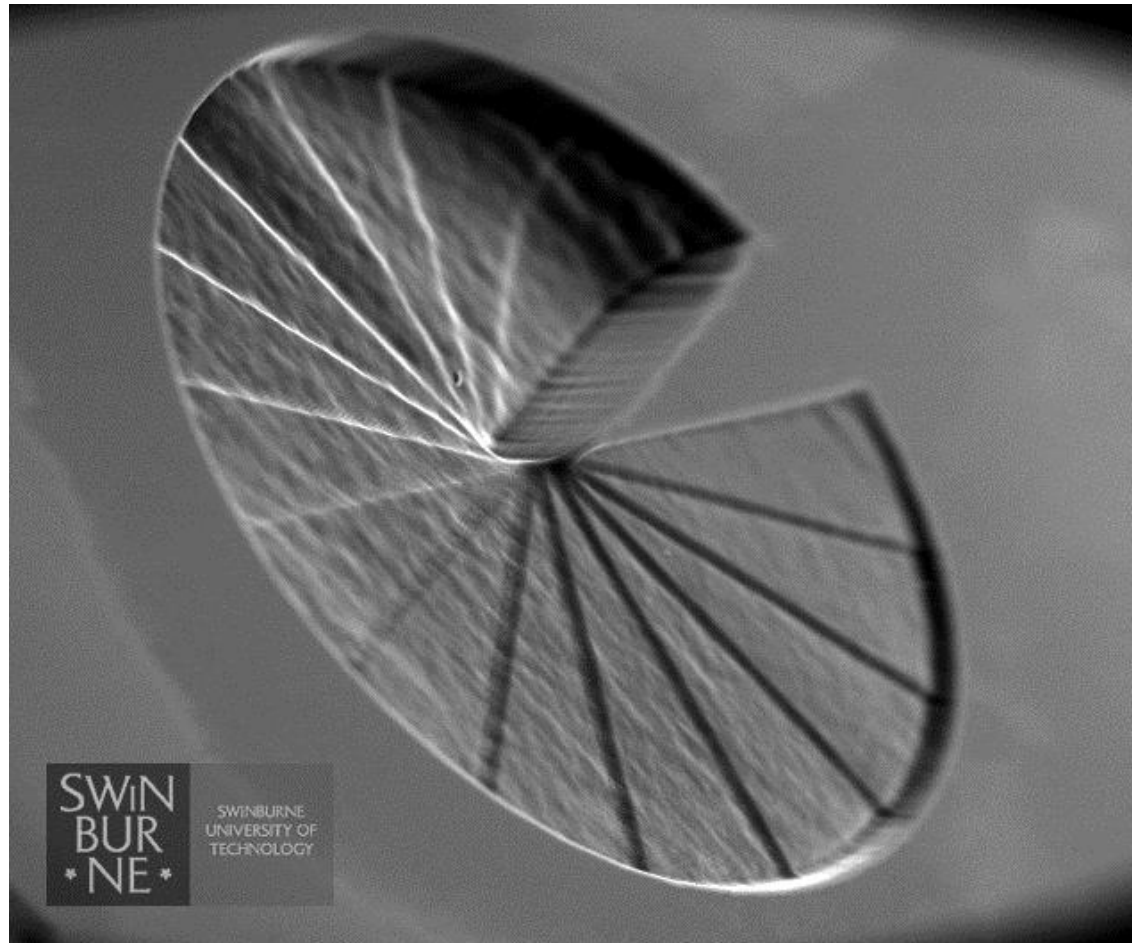
Means to generate the helical phase

Means to detect it

Will it be stable upon propagation, or fall apart due to rapidly varying phases and imperfect optics?



Spiral phase plate

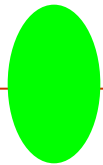
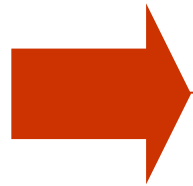


Polyimide phase plate, 34 μm thick, gives $\sim 2\pi$ shift at 9 keV



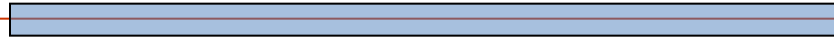
Experiment

Coherent x-ray beam

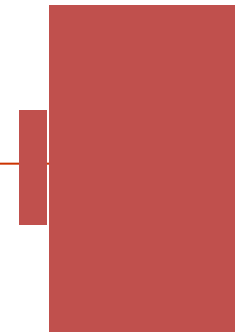


Spiral phase plate

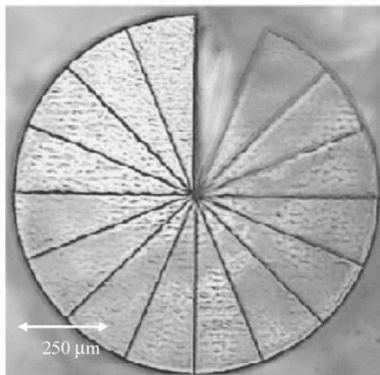
Helium flight path



CdWO₄ scintillator



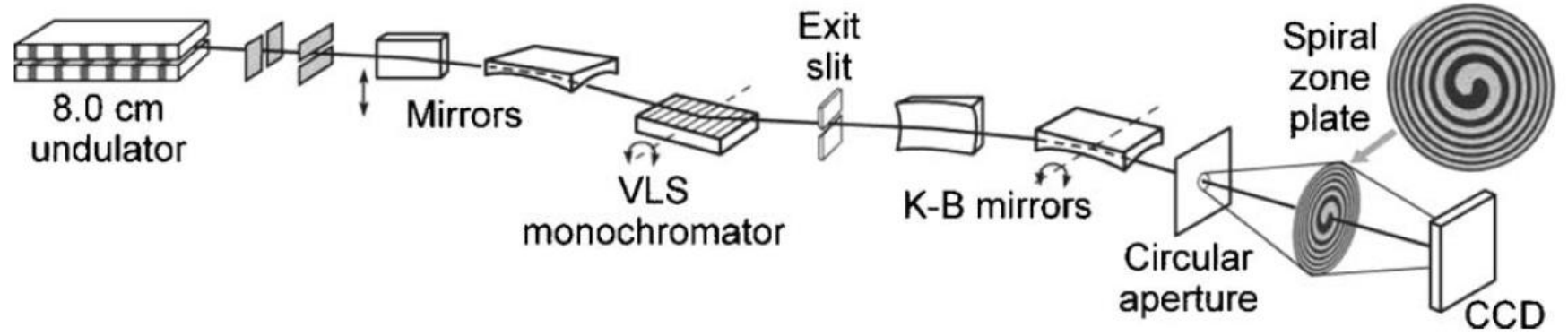
CCD camera



A. Peele, Opt. Lett. 27, 1752 (2002)



Spiral phase contrast x-ray microscopy



Images of 1 μm pinhole at $\lambda = 2.73 \text{ nm}$



ordinary ZP



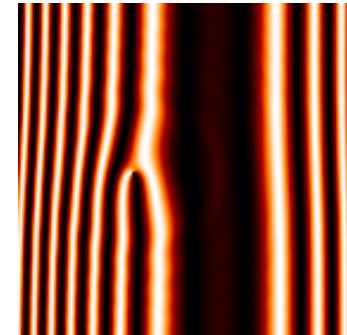
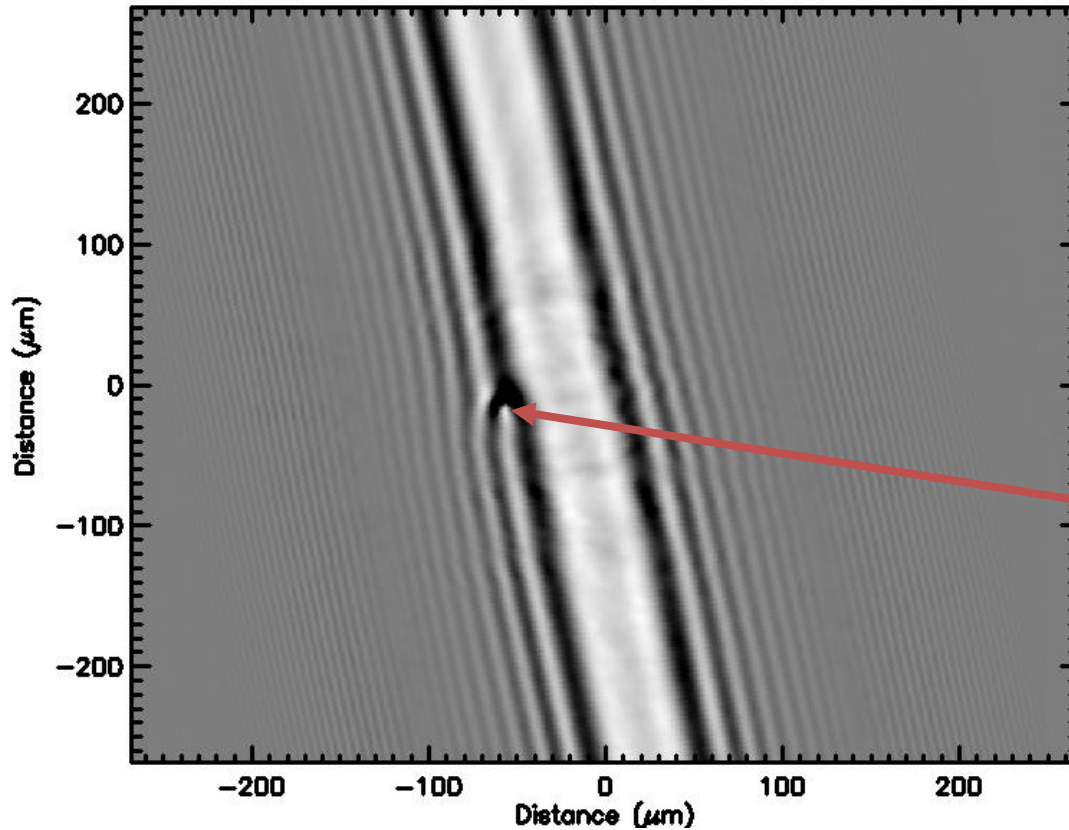
SZP, $l=1$



SZP, $l=2$



"Charge 1" vortex



$L = \hbar$
phase
singularity

Visualize singularity as split in Fresnel diffraction fringes from a tungsten wire (9 keV)



For a variable polarizing undulator with N periods (e.g. APPLE undulator), the radiated intensity of the n th harmonic is

$$\frac{d^2 I}{d\omega d\Omega} = \frac{e^2 \gamma^2 n^2 \xi^2}{4\pi \epsilon_0 c} \left[|A_x|^2 + |A_y|^2 \right] L(N\Delta\omega / \omega_1),$$

where:

$$A_x = 2\gamma\theta \cos \phi S_0 - K_y (S_1 + S_{-1})$$

$$A_y = 2\gamma\theta \sin \phi S_0 + iK_x (S_1 - S_{-1})$$

$$S_q = \sum_{p=-\infty}^{\infty} J_p(Y) J_{n+2p+q}(X) e^{i(n+2p+q)\Phi}$$

$L(N\Delta\omega/\omega_1)$ is the Laue function for fundamental ω_1 and $\Delta\omega = \omega - n\omega_1(\theta)$

$$q = -1, 0, 1$$

$$X = 2n\xi\gamma\theta \sqrt{K_y^2 \cos^2 \phi + K_x^2 \sin^2 \phi}$$

$$Y = n\xi(K_y^2 - K_x^2)/4, \quad \tan \Phi = (K_y / K_x) \tan \phi$$

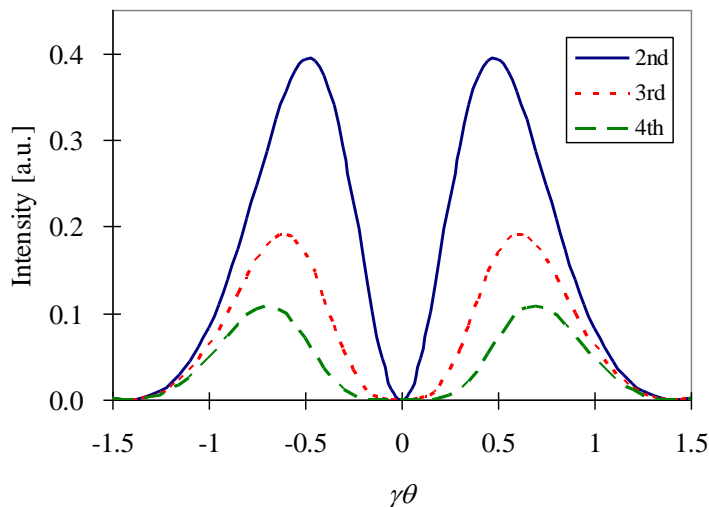
$$\xi = 1/(1 + \gamma^2 \theta^2 + K_x^2/2 + K_y^2/2)$$

B. Kincaid, JAP 48, 2684 (1977)
R. Walker, CERN Acc. School, 1998

For the pure circular mode, $K_y=K_x=K$ and $X=2n\xi\gamma\theta K$, $Y=0$, $\Phi=\phi$. After simple manipulation, we obtain

$$A_x = e^{in\phi} \left\{ 2\gamma\theta \cos \phi J_n(X) - K \left(J_{n+1}(X)e^{i\phi} + J_{n-1}(X)e^{-i\phi} \right) \right\}$$

$$A_y = e^{in\phi} \left\{ 2\gamma\theta \sin \phi J_n(X) - iK \left(J_{n+1}(X)e^{i\phi} - J_{n-1}(X)e^{-i\phi} \right) \right\}$$



To explore whether the higher harmonics carry OAM in general, we consider the time-independent complex amplitude. For the circular mode this can be written as → NEXT SLIDE

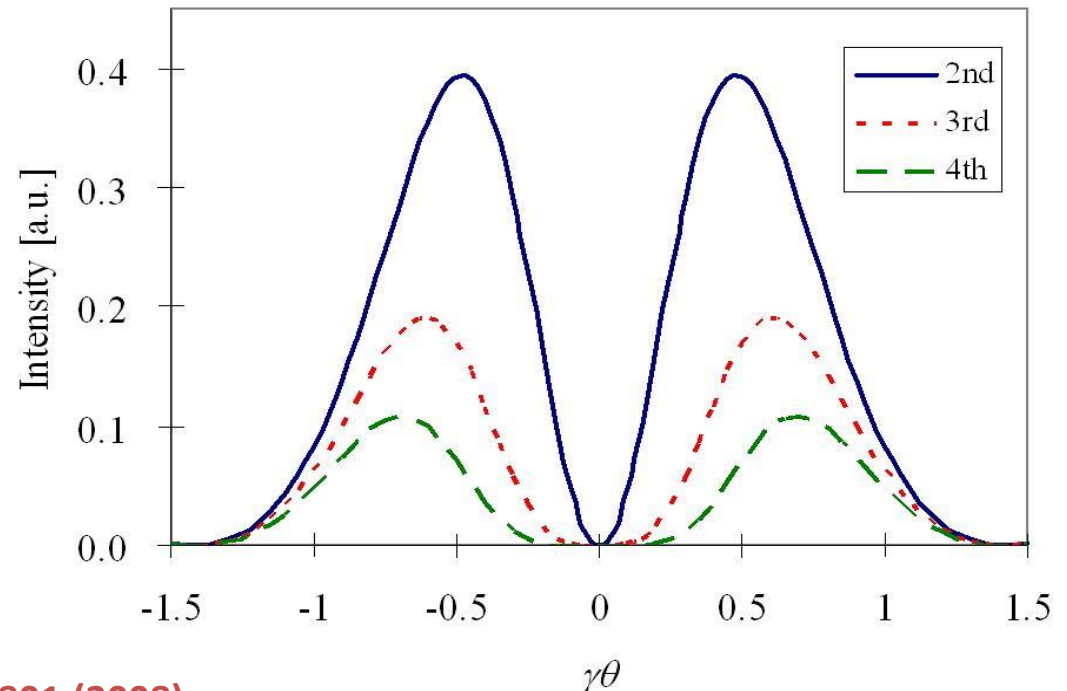
S. Sasaki, PAC07 Proc. TUPMN097, 2007

S. Sasaki, Nucl. Instrum. Methods A582 (2007) 43.

In this mode, $K_x = K_y = K$, $X = 2n\zeta\gamma\theta K$, $Y = 0$, and $\Phi = \phi$.

$$A = \frac{A_x - iA_y}{2} = \sqrt{2} e^{i(n-1)\phi} \left\{ \gamma\theta J_n(X) - J_{n-1}(X) \right\}$$

Radiated amplitude has the characteristic central minimum and $\exp(i\ell\phi)$ signature of LG modes





Comparisons between two equations

In the circular mode; $K_x = K_y = K$, $X = 2n\xi\gamma\theta K$, $Y = 0$, and $\Phi = \phi$.

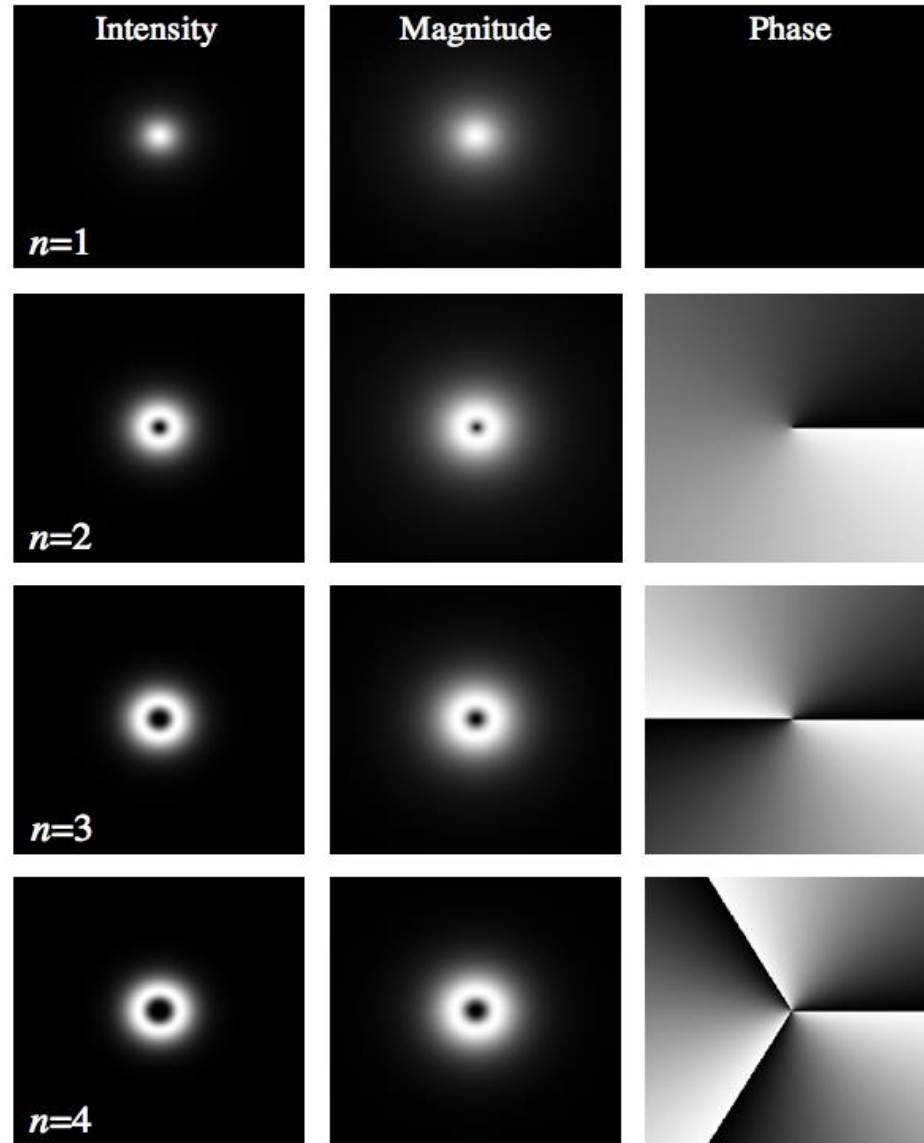
$$(A_x - iA_y)/2 = \sqrt{2} e^{i(n-1)\phi} \{\gamma\theta J_n(X) - J_{n-1}(X)\}$$

In Laguerre-Gaussian beam;

$$a_p^\ell(r, \phi, z) = A_p^\ell(r, z) \exp[-i\Phi_p^\ell(r, z)] \exp(-i\ell\phi)$$

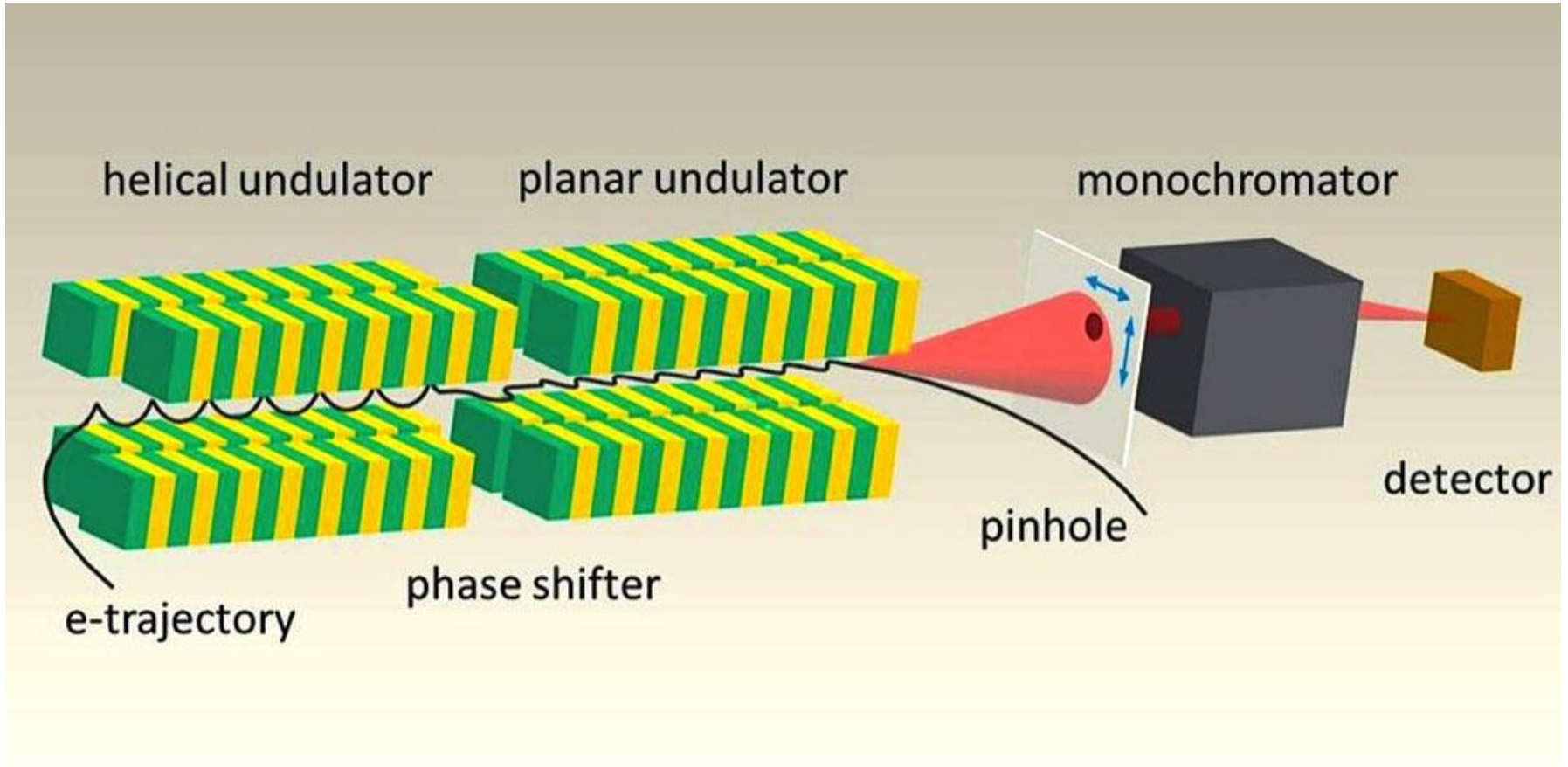


Intensity, magnitude, and phase for the first few harmonics





First Observation of OAM in Undulator Radiation



J. Bahrtdt, *et. al.* Phys. Rev. Lett. **111**, 034801 (2013).

First Observation of Light Vortices in Undulator Radiation

PRL **111**, 034801 (2013)

PHYSICAL REVIEW LETTERS

week ending
19 JULY 2013

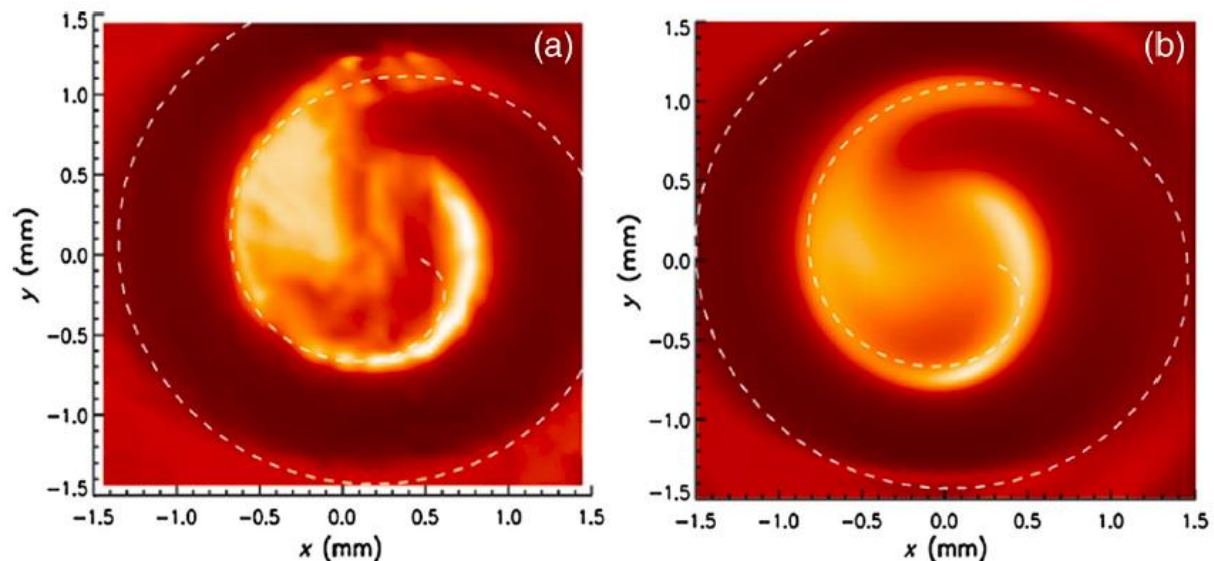
First Observation of Photons Carrying Orbital Angular Momentum in Undulator Radiation

J. Bahrtdt, K. Holldack, P. Kuske, R. Müller, M. Scheer, and P. Schmid
Helmholtz-Zentrum Berlin, Albert-Einstein-Straße 15, 12489 Berlin, Germany
(Received 26 February 2013; published 15 July 2013)

Photon beams of 99 eV energy carrying orbital angular momentum (OAM) have been observed in the 2nd harmonic off-axis radiation of a helical undulator at the 3rd generation synchrotron radiation light source BESSY II. For detection, the OAM carrying photon beam was superimposed with a reference beam without OAM. The interference pattern, a spiral intensity distribution, was recorded in a plane perpendicular to the helicity of the beam. The helicity of the beam has been found.

DOI: [10.1103/P](https://doi.org/10.1103/PhysRevLett.111.034801)

Introduction.—For an exact solution of the Helmholtz equation can be expanded in Legendre polynomials. In 1992, Allen *et al.* demonstrated beams consisting of an l th order phase distribution and an angular momentum of lh . Numerous experiments using OAM beams were utilized for the micromanipulation of particles in optical tweezers [4] or for channel multiplexing in



A chicane converts this energy modulation into a helical



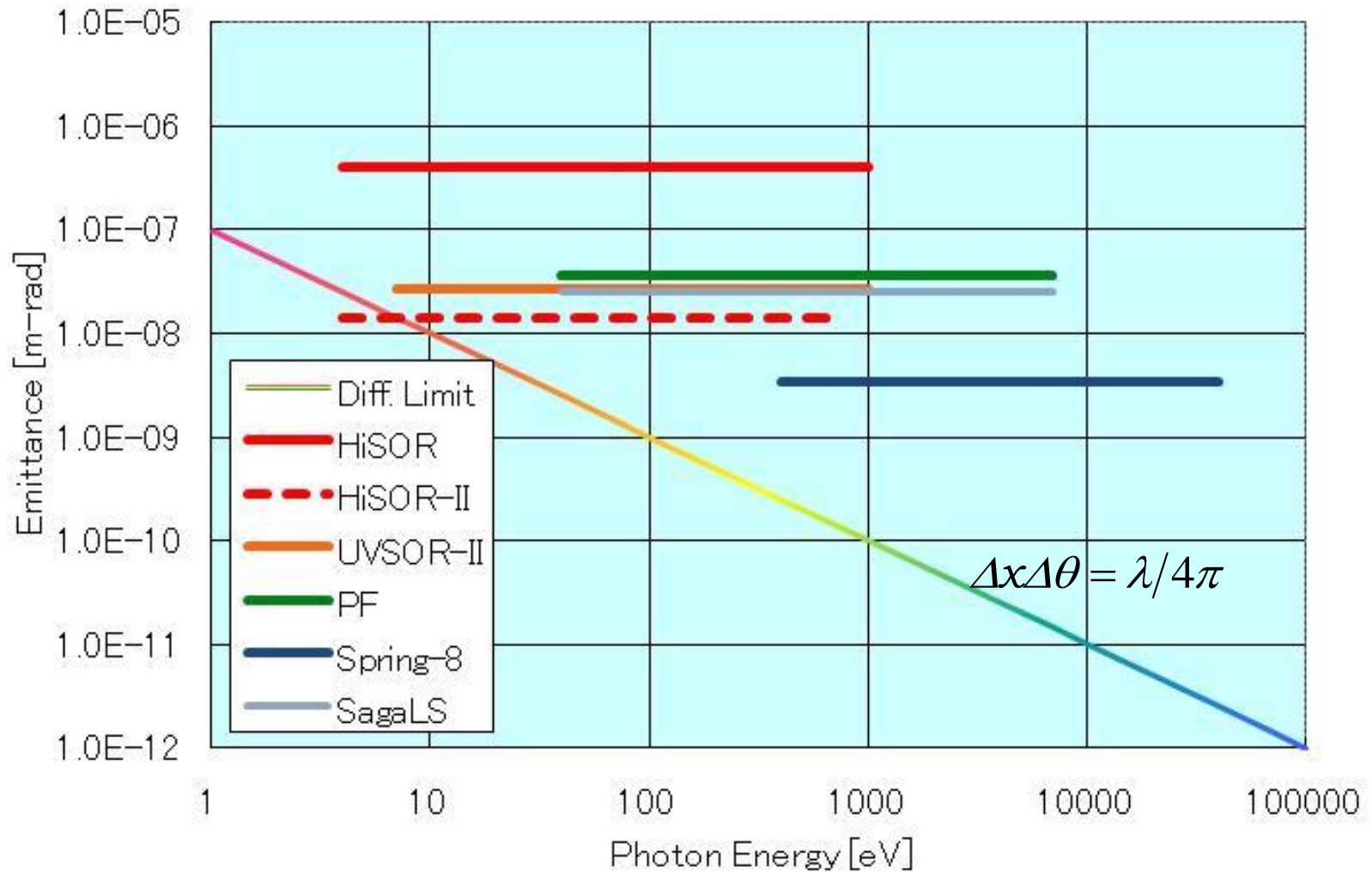
2010年時点の日本の光源リング

挿入光源が設置されている放射光源リングに限った

Facility	Energy [GeV]	Emittance
Spring-8	8	3.4
PF	2.5	36
SagaLS	1.4	25
NewSubaru	1-1.5	37
UVSOR-II	0.75	27
HiSOR	0.7	400
NagoyaLS	1.2	53
HiSOR-II	0.7	14
MAX III	0.7	13

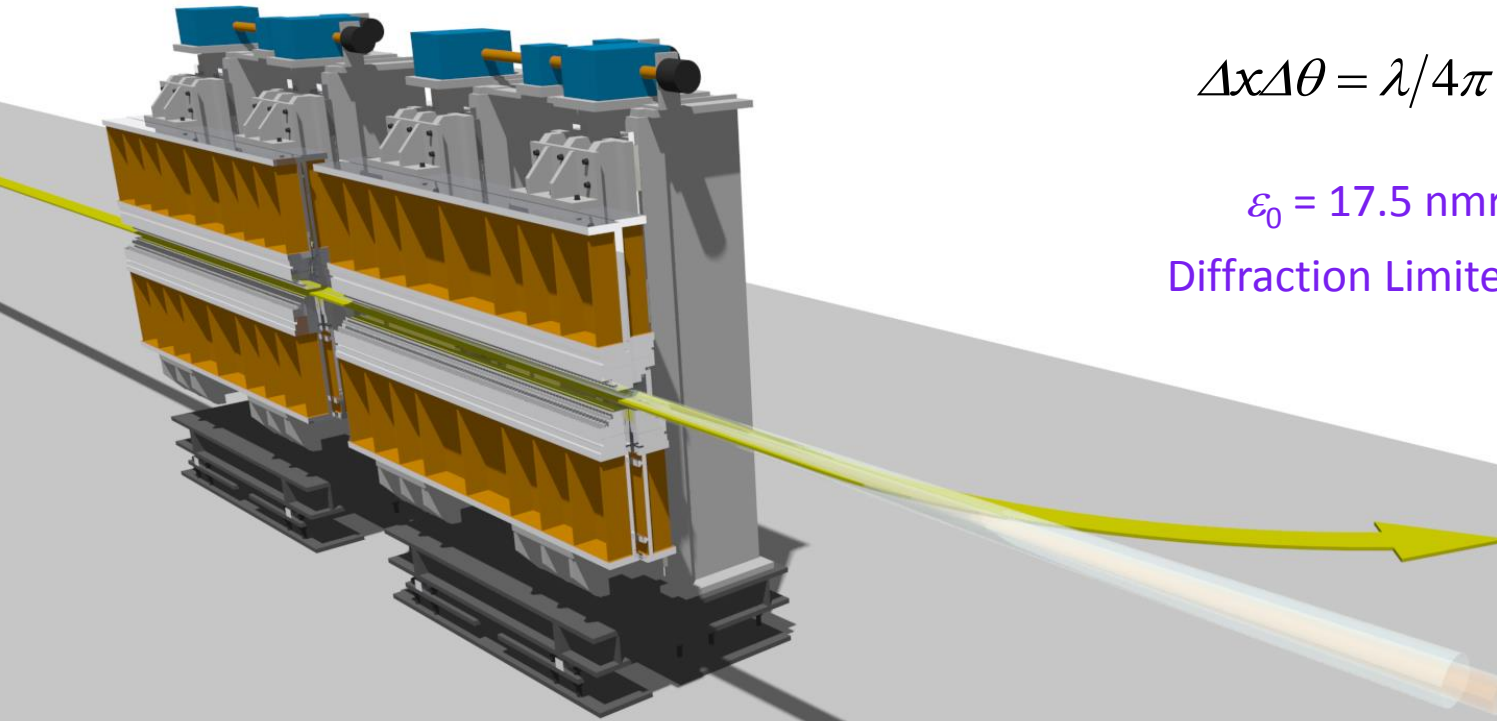


回折限界とエミッタンス





Experiments at UVSOR-III



$$\Delta x \Delta \theta = \lambda / 4\pi : 10 \text{ nmrad} \sim 10 \text{ eV}$$

$$\varepsilon_0 = 17.5 \text{ nmrad} @ 750 \text{ MeV}$$

Diffraction Limited LS below $E_p = 6 \text{ eV}$

750 MeV : Emittance = 17.5 nmrad, DL wavelength=220 nm, 6eV

600 MeV : Emittance = 10.9 nmrad, DL wavelength=138 nm, 9eV

500 MeV : Emittance = 7.6 nmrad, DL wavelength=100 nm, 12eV

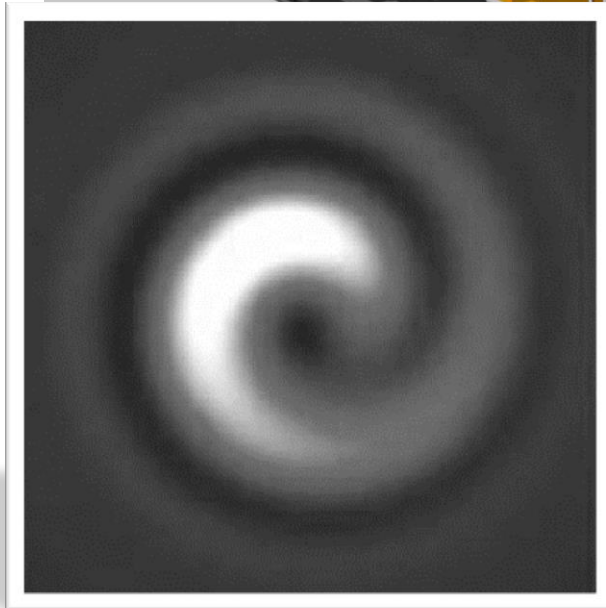
400 MeV : Emittance = 4.8 nmrad, DL wavelength=63 nm, 20eV

2台のアンジュレータ光の干渉

- 2次光と1次光の干渉を見ると
– 1本の渦巻きが見えるはず

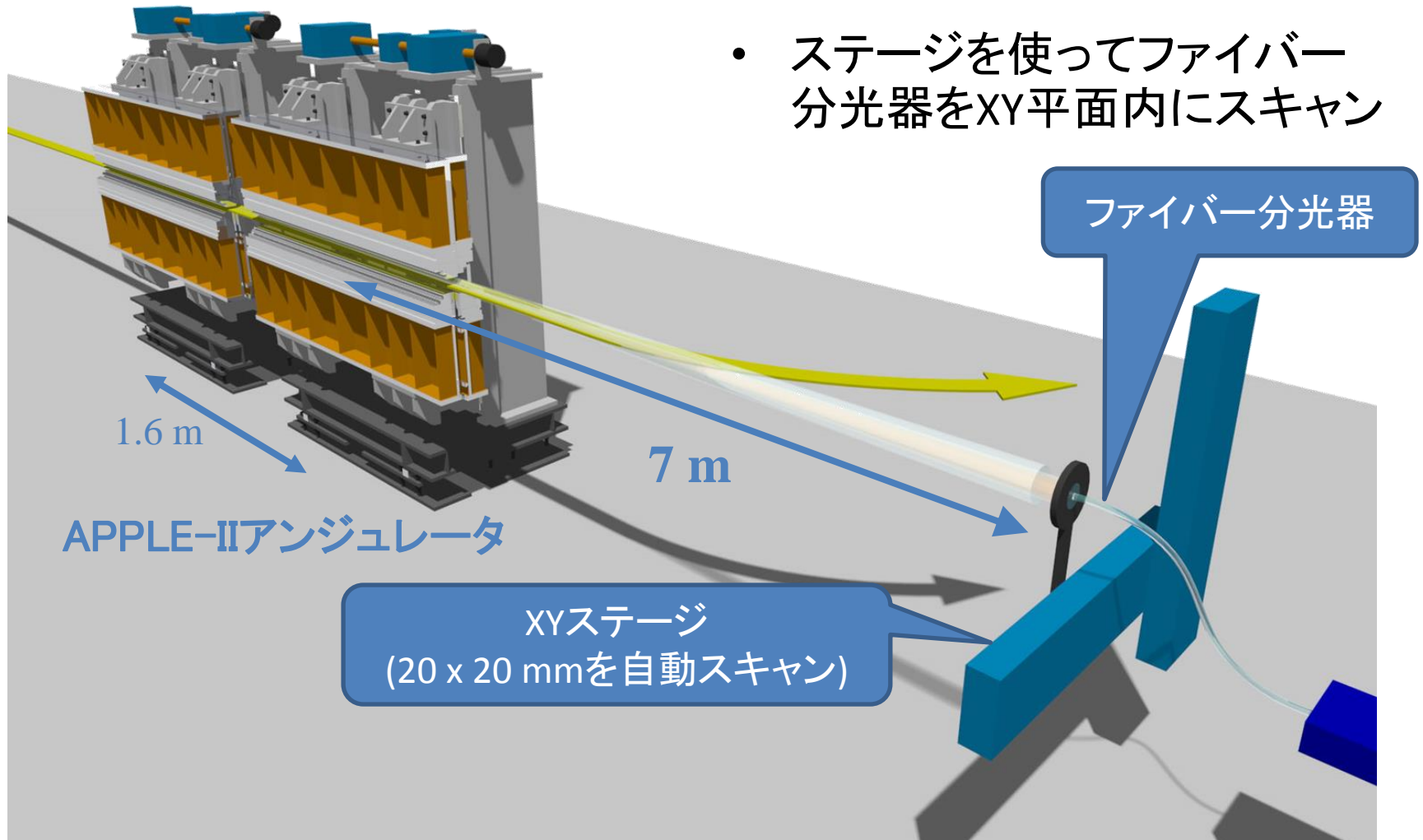
上流のアンジュレータ光
(1次光)

下流のアンジュレータ光
(2次光)



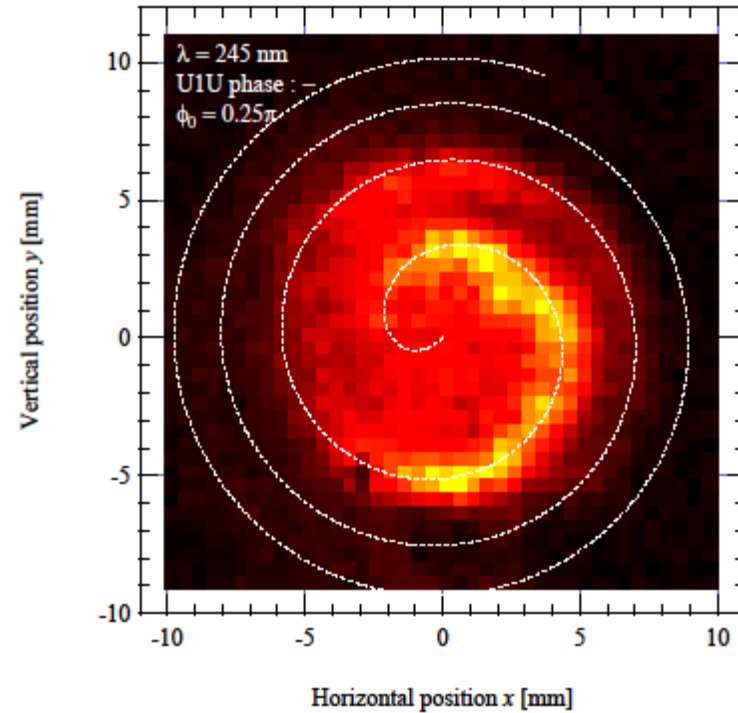
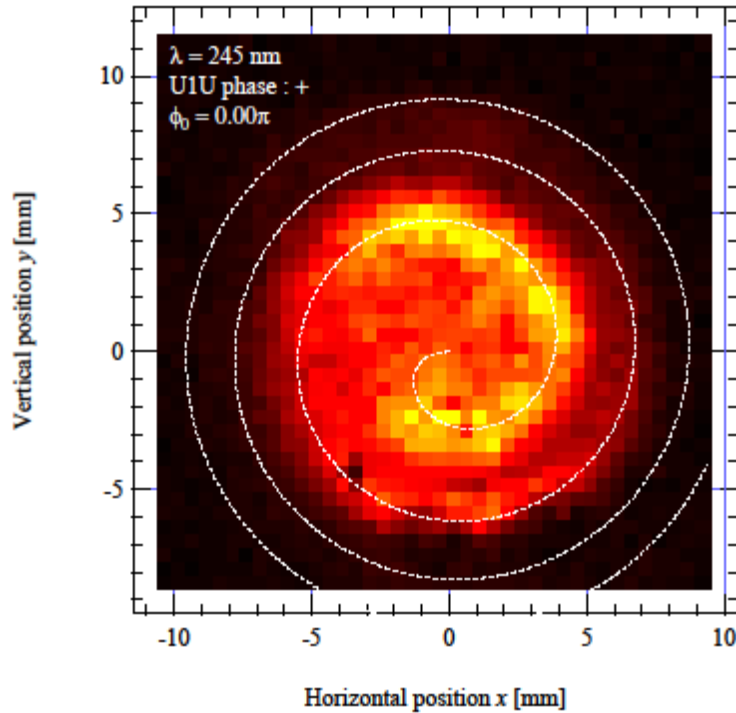
ファイバー分光器による観測

- ステージを使ってファイバー分光器をXY平面内にスキャン



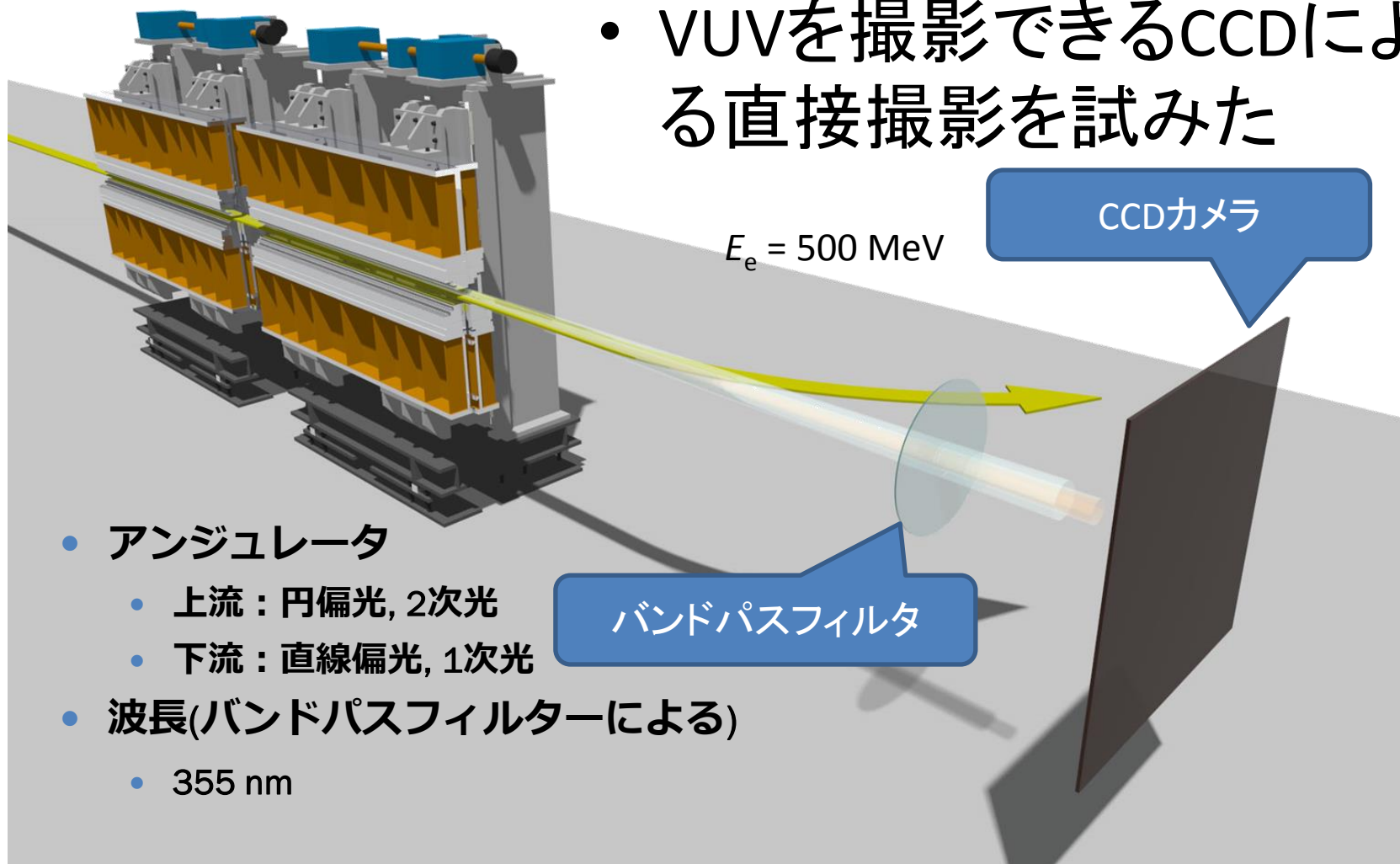
Results of Experiments

$E = 600 \text{ MeV}$, $\varepsilon_0 = 11 \text{ nmrad}$



CCDカメラによる観測

- VUVを撮影できるCCDによる直接撮影を試みた

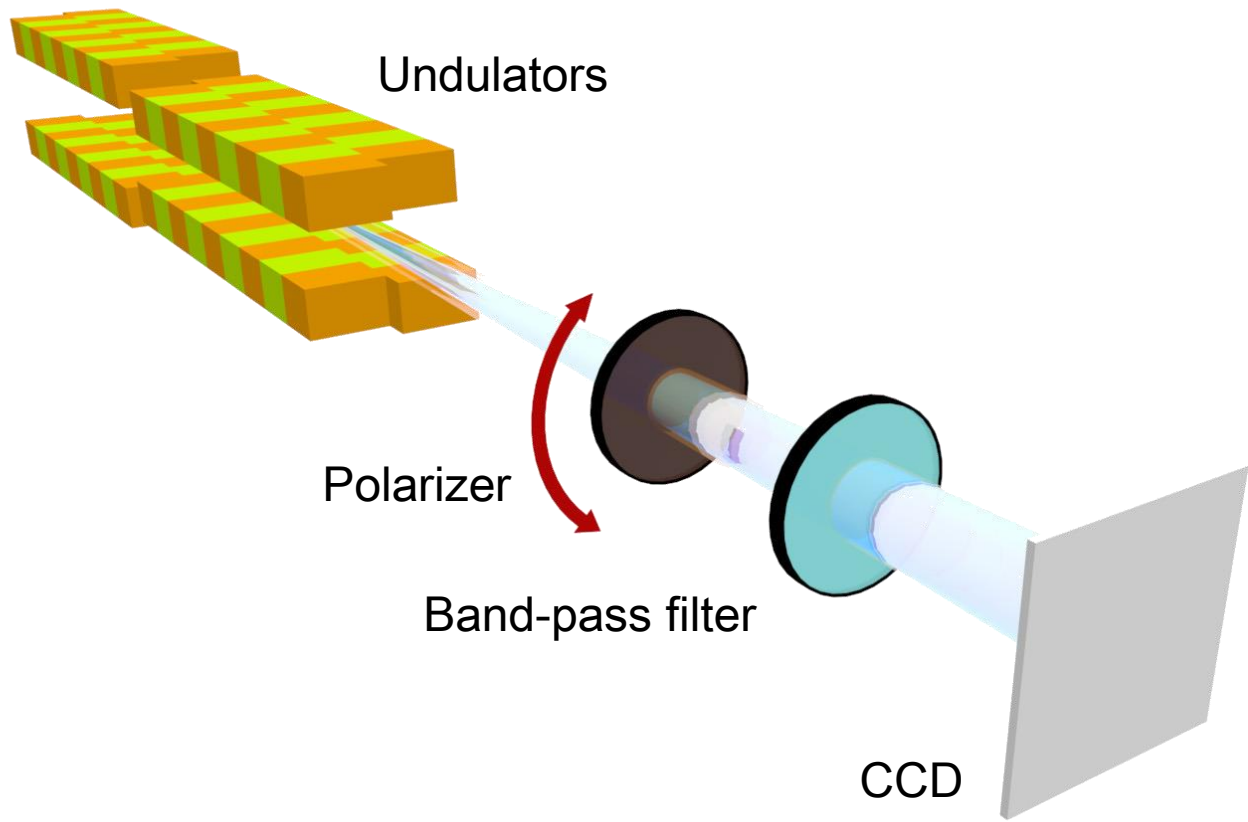


- アンジュレータ
 - 上流：円偏光, 2次光
 - 下流：直線偏光, 1次光
- 波長(バンドパスフィルターによる)
 - 355 nm

CCDカメラ

$E_e = 500 \text{ MeV}$

バンドパスフィルタ



Interferences between both circular polarizations

- 同符号のSを持つ円偏光

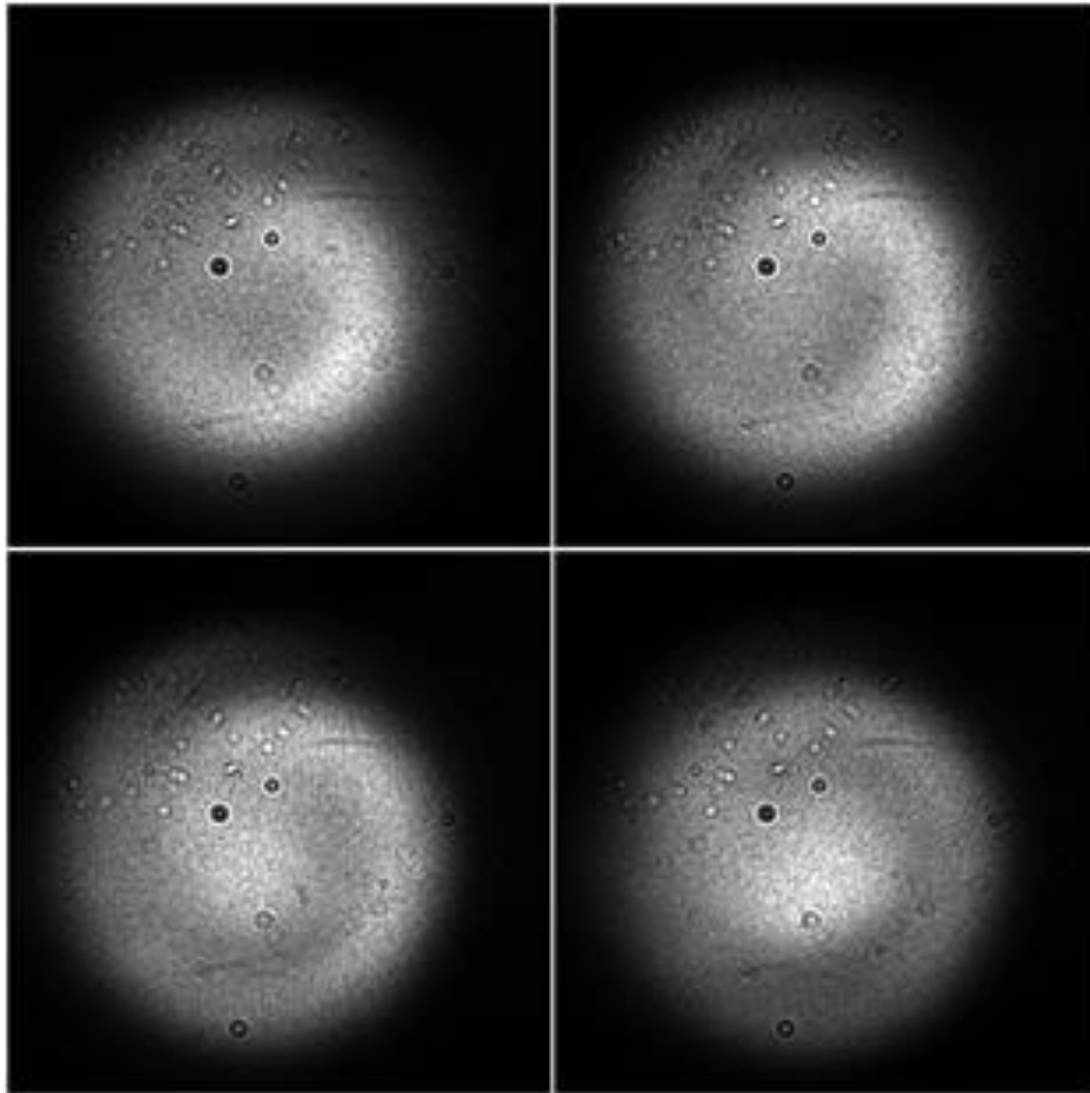
強め合う位置

偏光子を通して
方向の電場のみ
通過するようにすると？

光が強め合う位置は
時間的に変化しない

- 逆符号のSを持つ円偏光

時間的に積分すると
ドーナツ状に光る！

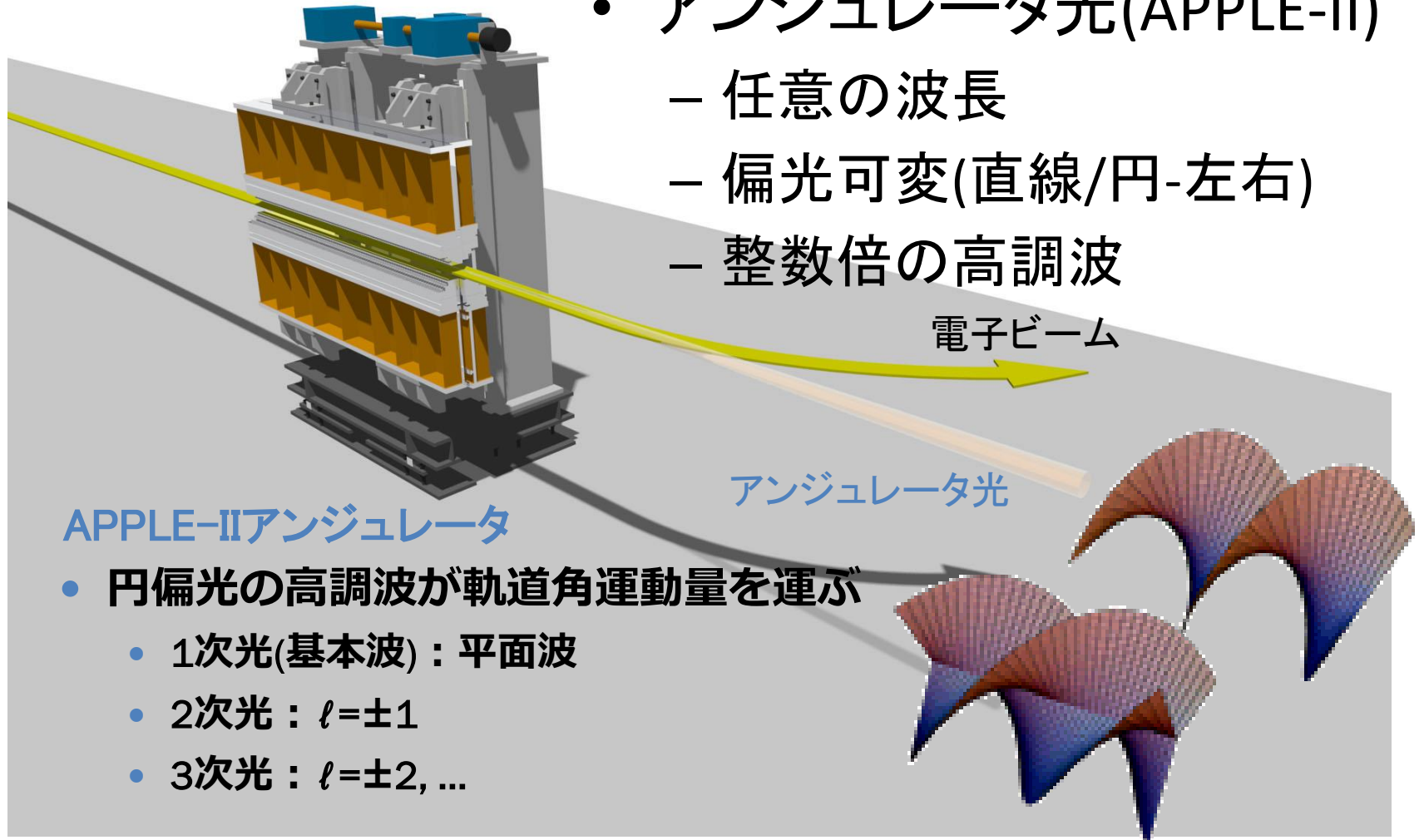


Circular 1st (upstream: $s=+1, \ell=0$) & 2nd harmonic (downstream: $s=-1, \ell=-1$) interference.

Measurements were done with a polarimeter. The spiral pattern rotates with the rotation of the polarimeter. $E = 600$ MeV, $e_0 = 11$ nrad, $l = 240$ nm. Rotation angles of the polarimeter are: Top Left: 0° , Top Right: 30° , Bottom Left: 60° , Bottom Right: 90°

OAMを持つアンジュレータ光

- アンジュレータ光(APPLE-II)
 - 任意の波長
 - 偏光可変(直線/円-左右)
 - 整数倍の高調波



APPLE-IIアンジュレータ

- 円偏光の高調波が軌道角運動量を運ぶ
 - 1次光(基本波) : 平面波
 - 2次光 : $l = \pm 1$
 - 3次光 : $l = \pm 2, \dots$

1次光と高次光の干渉による渦巻きパターン

- 上流アンジュレータからの放射光

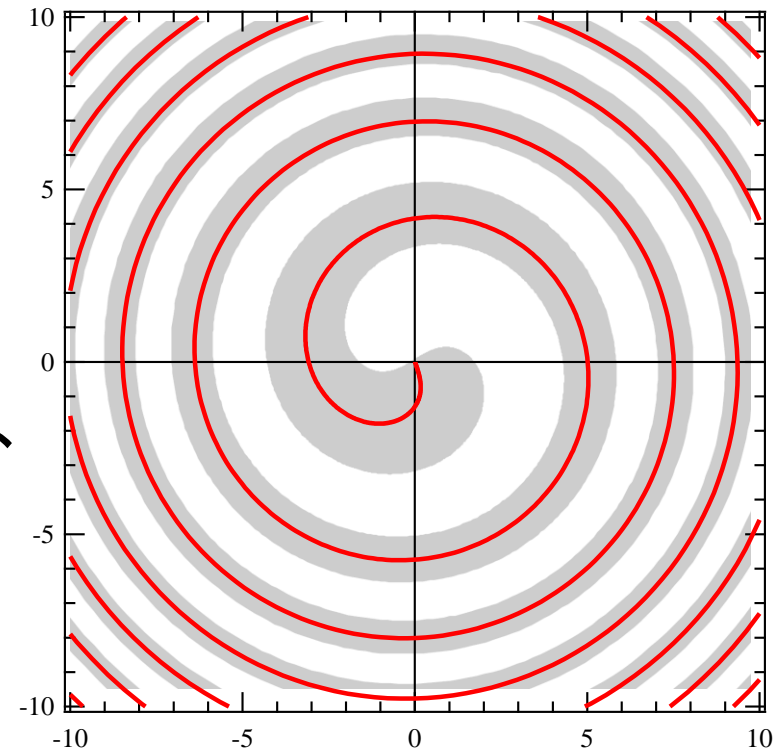
$$A(r, \varphi) = \frac{a(r)}{L+d} \cos\left(\frac{\pi d}{\gamma^2 \lambda} + \frac{\pi}{(L+d)\lambda} r^2 \pm (n-1)\varphi + \frac{2\pi L}{\lambda} - \omega t\right)$$

- 下流アンジュレータ

$$B(r, \varphi) = \frac{b(r)}{L} \cos\left(\frac{\pi}{L\lambda} r^2 + \frac{2\pi L}{\lambda} - \omega t\right)$$

- $A + B$ を $0 \sim \omega/2\pi$ の間 t で積分して
cos関数の中身が0になる φ は、

$$\varphi = \pm \left(-\frac{\pi d}{\gamma^2 \lambda} + \frac{\pi d}{L^2 \lambda} r^2 \right) / (n-1)$$

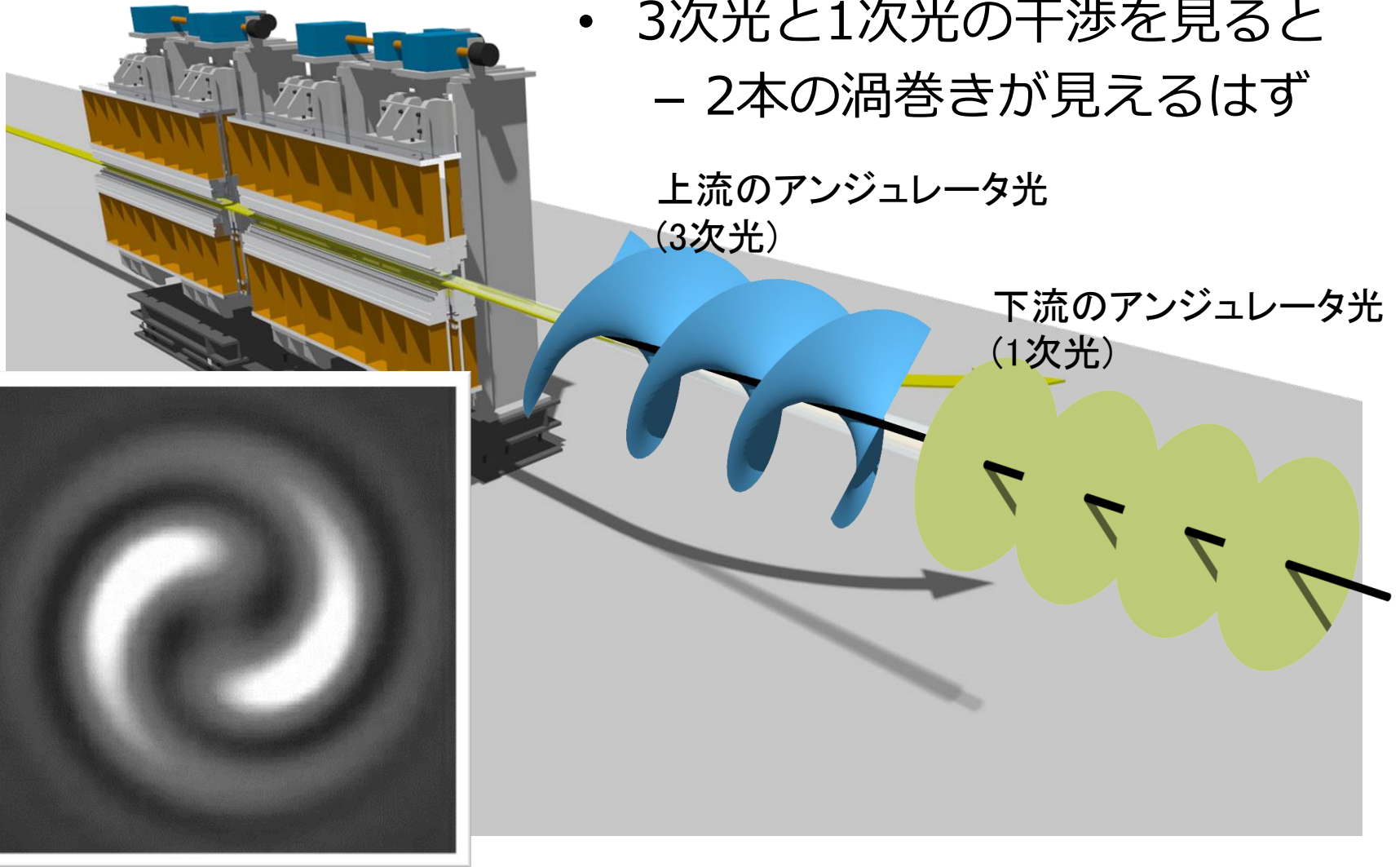
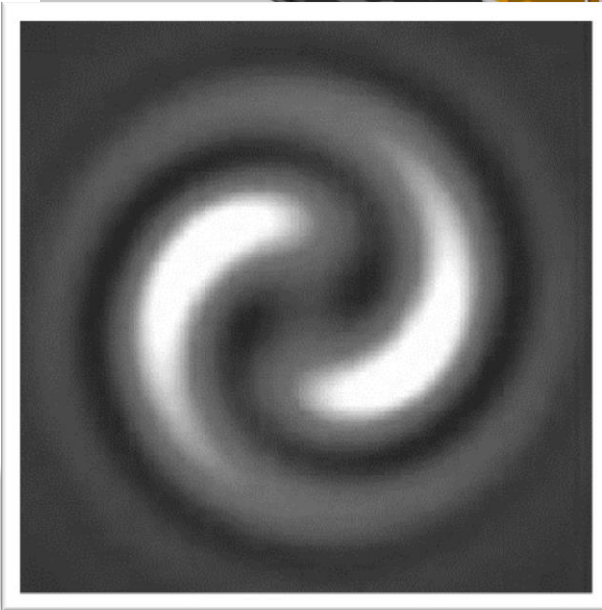


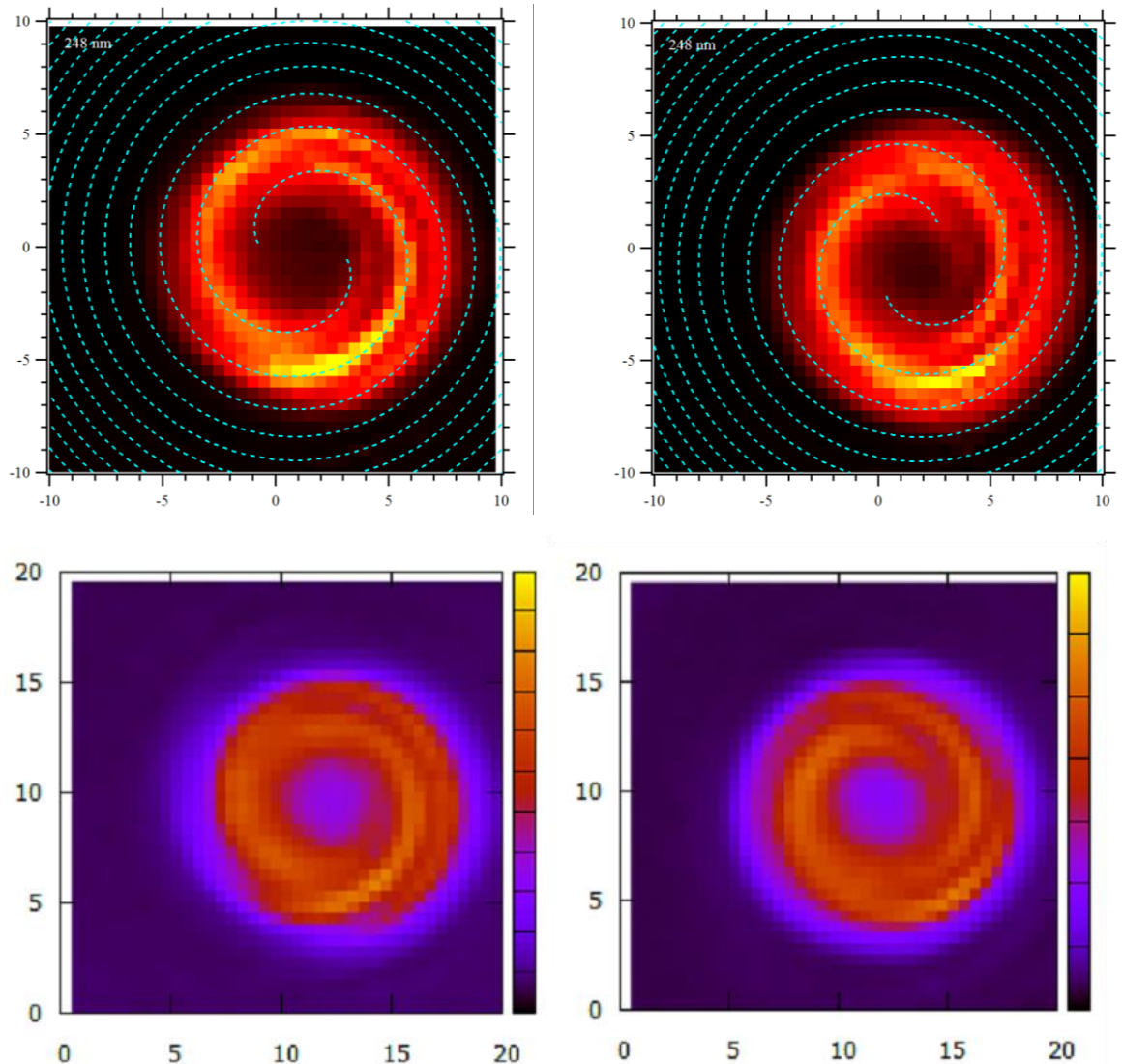
3次の光で見ると...

- 3次光と1次光の干渉を見ると
– 2本の渦巻きが見えるはず

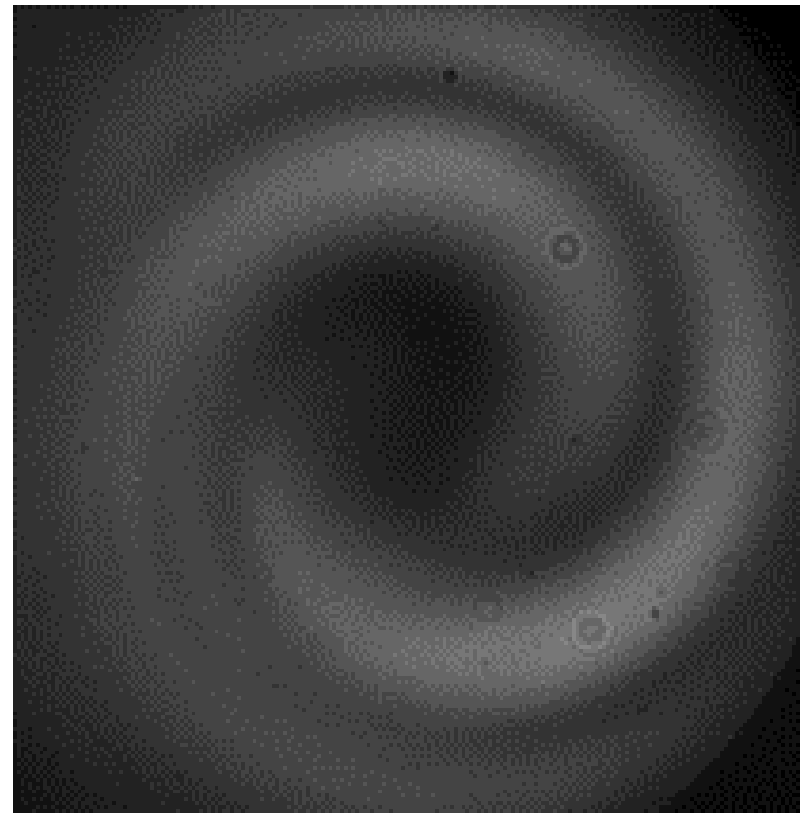
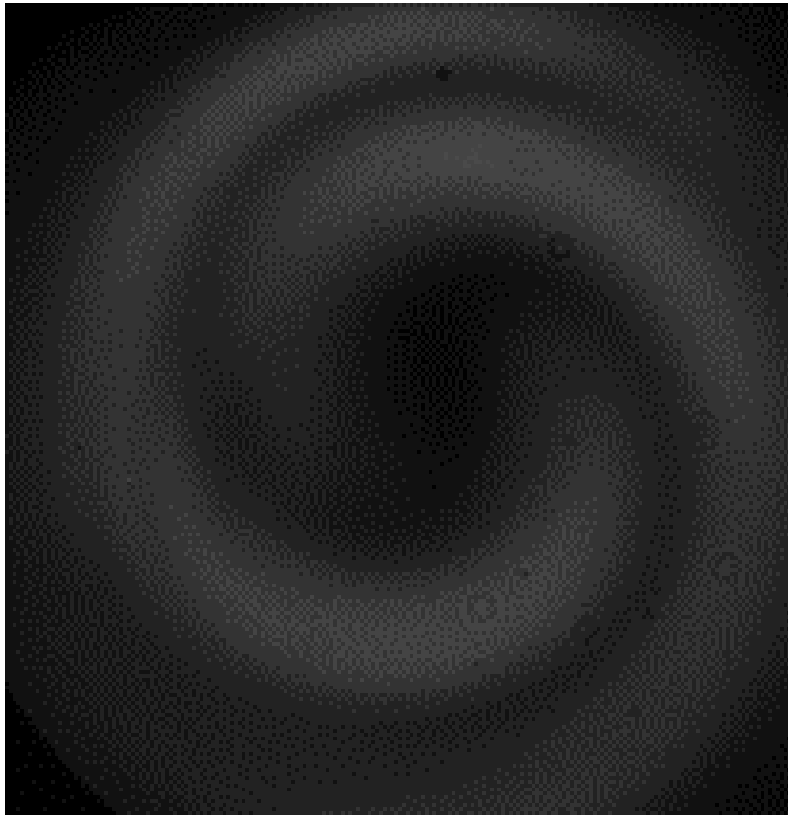
上流のアンジュレータ光
(3次光)

下流のアンジュレータ光
(1次光)



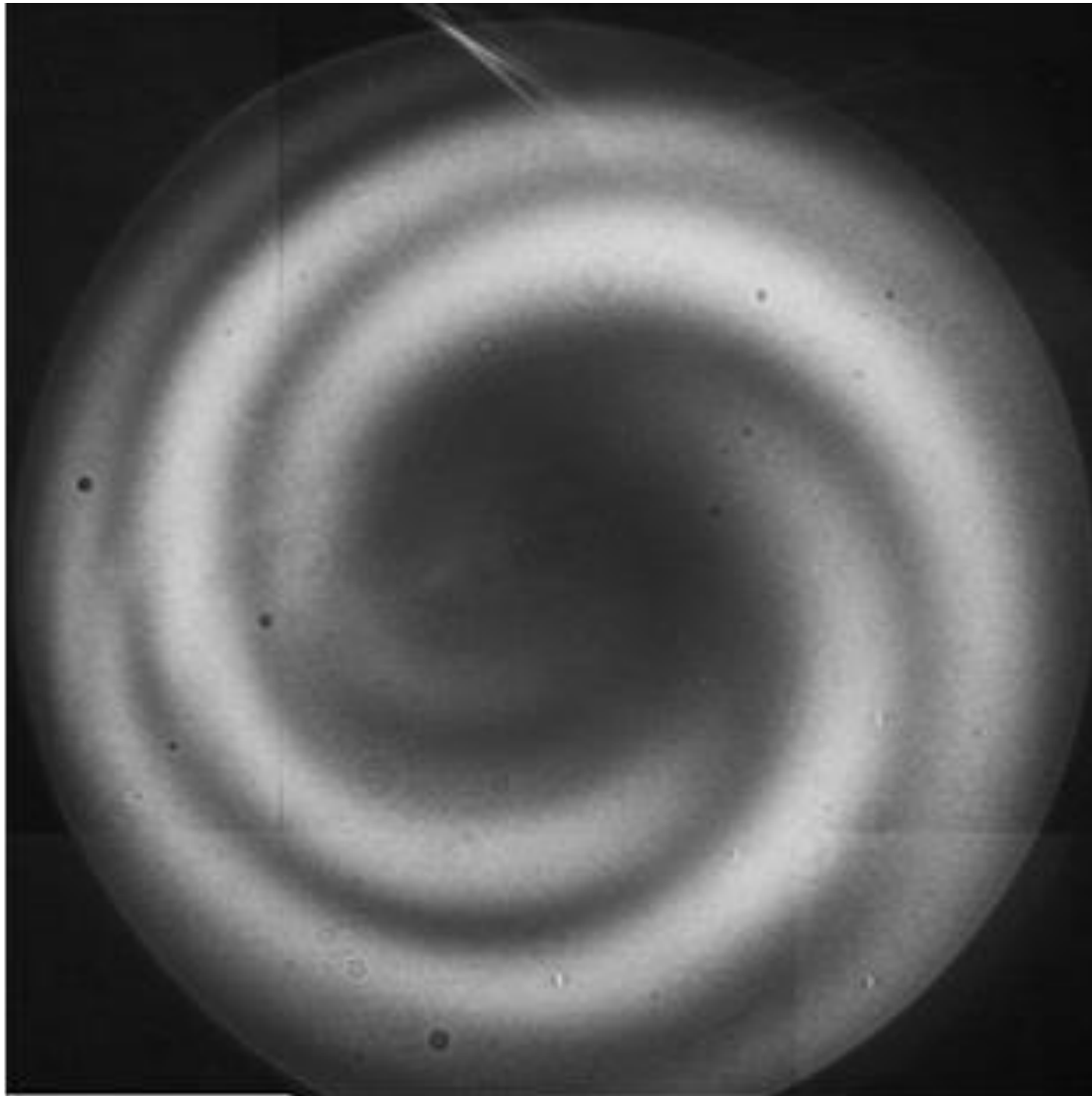


Double spiral by linear 1st & circular 3rd harmonic (Top row) and that by the circular 1st & 3rd harmonic with the same helicity interference (Bottom row). $E = 500$ MeV, $e_0 = 8$ nmrad, $l = 248$ nm, downstream undulator setting: left column; $s=-1, \ell=-2$, rightcolumn; $s=+1, \ell=+2$, without a polarimeter.



Double spiral by 2nd ($\ell=\pm 1$) & 2nd ($\ell=\mp 1$) harmonic interference.

$E = 500$ MeV, $\varepsilon_0 = 8$ nmrads, $l = 355$ nm, with a polarimeter.



Triple spiral by the circular 2nd ($s=+1, \ell=+1$) and 3rd ($s=-1, \ell=-2$) harmonic interference.
 $E = 400$ MeV, $\varepsilon_0 = 5$ nmrاد, $\lambda = 355$ nm, with a polarimeter (band width $\Delta\lambda = 1.3$ nm).

X-ray orbital dichroism

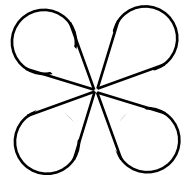
- Dichroic effects are expected with x-ray beams carrying OAM.
- Sensitive to DOS occupancy difference between orbitals with $j \pm \ell$ and $j = 0$.
- Enables study of unoccupied states in absence of strong core-hole effects.
- Subtracting spectra measured with \pm OAM states allows separation of quadrupolar from much stronger dipolar transitions. e.g.,

$$\mathbf{A}_\ell(\mathbf{r}) = \hat{\mathbf{e}}_\ell A_\ell \left(\frac{\rho}{w} \right)^{|\ell|} \exp(i\ell\phi + ikz)$$

$$\left\langle f \left| \frac{e}{m} \mathbf{p} \cdot \mathbf{A}(\mathbf{R} + \mathbf{r}) \right| g \right\rangle$$

Probe $\Delta j = \pm 2$ transitions
(e.g. 3d \rightarrow 1s) in:

- cuprates
- manganites
- ruthenates
- rare-earths

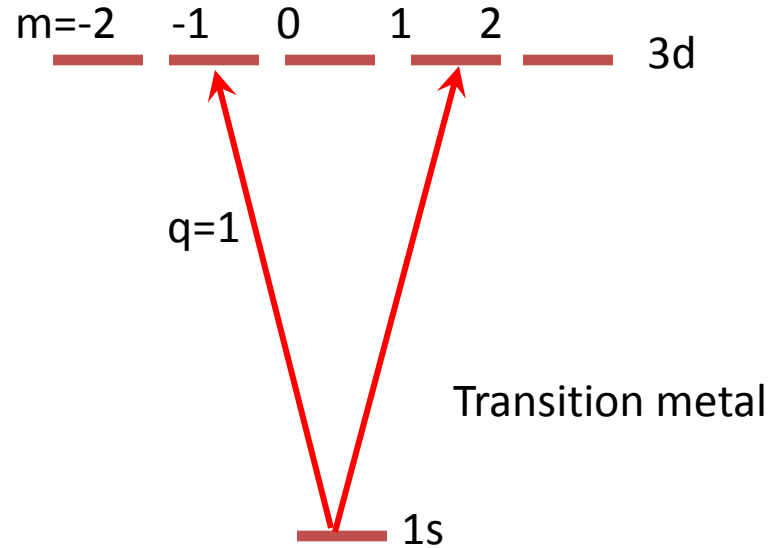
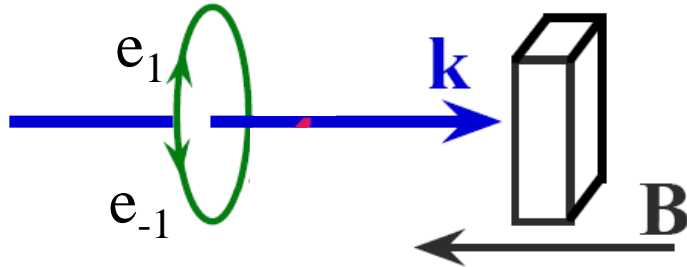


But: cross-section scales as $(\rho/w)^{|\ell|}$!

A. Alexandrescu, PRL 96, 243001 (2006)

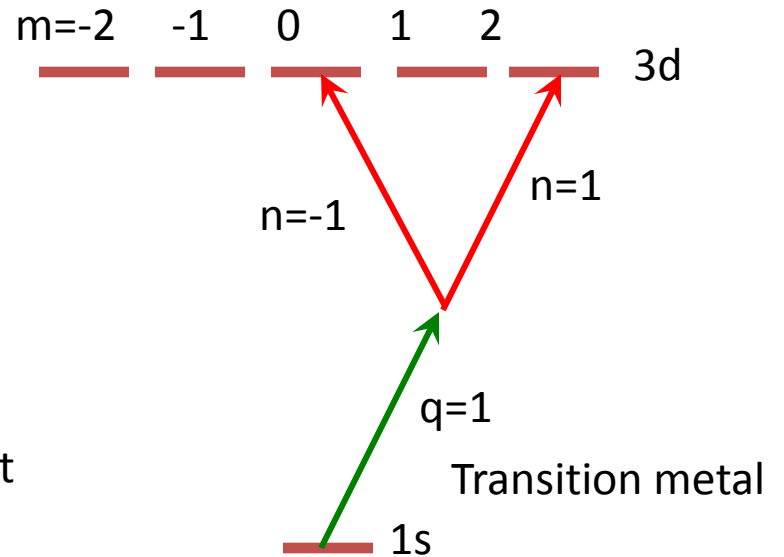
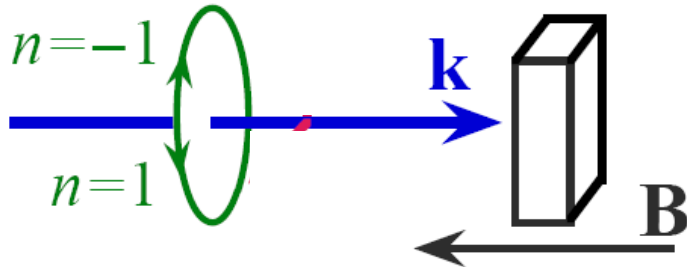
Conventional dichroism

subtract spectra with left and right polarized light



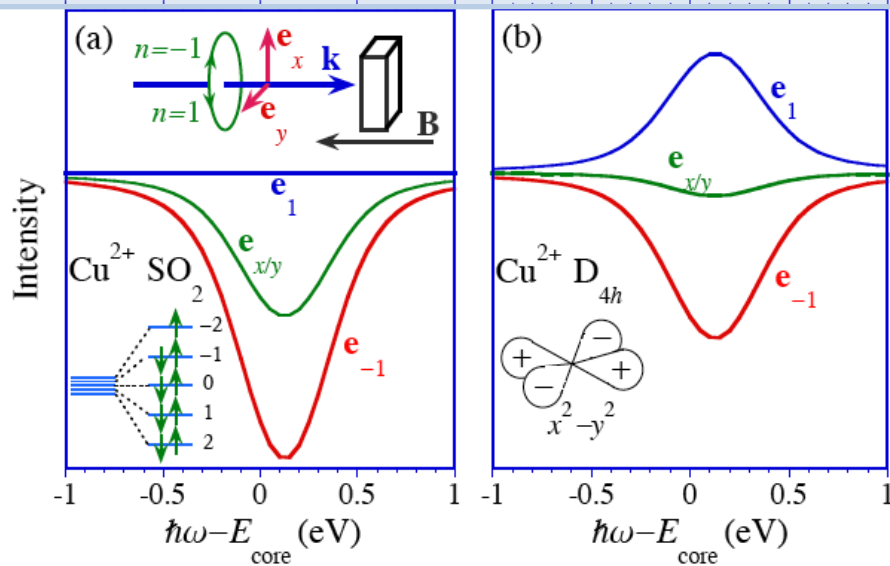
"Orbital dichroism"

subtract spectra with positive and negative orbital angular momentum of the beam

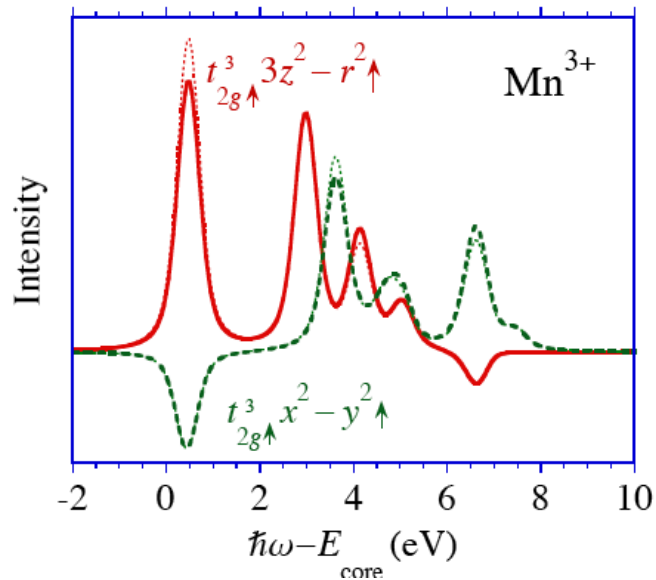


Use left ($q = 1$) circularly polarized light

Predicted spectra



(a) OAM dichroic signal using circularly (e_1, e_{-1}) and linearly ($e_{x/y}$) polarized x-rays for a Cu^{2+} ion in spherical symmetry and z-axis B-field. (b) Cu^{2+} ion in crystal field with D_{4h} symmetry.



OAM dichroism spectrum of Mn^{3+} ion.

van Veenendaal and McNulty, PRL (2007)

まとめ

- **軌道角運動量を持つアンジュレータ放射光**
回折限界光条件での検証実験@UVSOR-III
 - 2次光と1次光、3次光と1次光の干渉による渦巻の観測を行った。
 - ℓ の符号による回転方向の違いも確認
 - 1次光のヘリシティを逆転した観測も行った。
 - 逆ヘリシティの場合、偏光子を回転すると干渉パターンも回転した
 - 逆ヘリシティの2次光どうし、2次光と3次光の干渉も観測した。
 - 新しい放射光利用研究のプローブとなる可能性を秘めている。